

Neutral High-Potential Nickel Triad Bis(dithiolenes): Structure and Solid-State NMR Properties of $\text{Pt}[\text{S}_2\text{C}_2(\text{CF}_3)_2]_2$ Elzbieta Kogut,[†] Joel A. Tang,[‡] Alan J. Lough,[§] Cory M. Widdifield,[‡] Robert W. Schurko,^{*,‡} and Ulrich Fekl^{*,†}*Department of Chemical and Physical Sciences, UTM, 3359 Mississauga Road North, University of Toronto, Mississauga, Ontario, Canada L5L 1C6, Department of Chemistry & Biochemistry, University of Windsor, Windsor, Ontario, Canada N9B 3P4, and X-ray Crystallography, University of Toronto, 80 St. George Street, Toronto, Ontario, Canada M5S 3H6*

Received August 8, 2006

X-ray crystallography and solid-state NMR techniques were used to determine the structure and ^{195}Pt NMR chemical shift (CS) tensor of $\text{Pt}[\text{S}_2\text{C}_2(\text{CF}_3)_2]_2$. This is the first reported crystal structure of a highly oxidizing (CN- or CF_3 -substituted) neutral bis(dithiolene) complex of a Ni triad metal in its pure form. The ^{195}Pt NMR CS tensor is highly anisotropic and asymmetric; the latter property is attributed to the noninnocent nature of the ligand. The tensor components and orientation are determined with density functional theory calculations.

The bis(dithiolene) complexes of the Ni triad (group 10), $\text{M}[\text{S}_2\text{C}_2\text{R}_2]_2^z$ ($\text{M} = \text{Ni, Pd, Pt}$; $\text{R} =$ various substituents; charge $z = 0, 1-, 2-$), contain redox-active (noninnocent) ligands.¹ The ligand properties are crucial for applications such as superconducting materials,^{1h} photonic devices,^{1f–h} chemical sensors,^{1g} catalysts, and catalyst precursors.^{1e} The noninnocent nature of the ligand becomes particularly evident when the charge-neutral form ($z = 0$) is considered, where possible resonance structures involve metal oxidation states ranging from 0 to IV (Scheme 1). It is now well established that the metal is best described as M^{II} .^{1c}

* To whom correspondence should be addressed. E-mail: rschurko@uwindsor.ca (R.W.S.), ufekl@utm.utoronto.ca (U.F.).

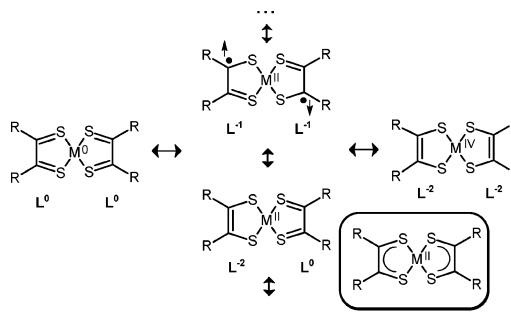
[†] Department of Chemical and Physical Sciences, UTM, University of Toronto.

[‡] University of Windsor.

[§] X-ray Crystallography, University of Toronto.

- (1) Dithiolene Chemistry: Synthesis, Properties, and Applications. In *Progress in Inorganic Chemistry*; Stiefel, E. I., Ed.; John Wiley and Sons: Hoboken, NJ, 2004; Vol. 52. Chapters of this book that are relevant in the present context: (a) Rauchfuss, T. B. Synthesis of Transition Metal Dithiolenes, p 1. (b) Beswick, C. L.; Schulman, J. M.; Stiefel, E. I. Structures and Structural Trends in Homoleptic Dithiolene Complexes, p 55. (c) Kirk, M. L.; McNaughton, R. L.; Helton, M. E. The Electronic Structure and Spectroscopy of Metallo–Dithiolene Complexes, p 111. (d) Johnson, M. K. Vibrational Spectra of Dithiolene Complexes, p 213. (e) Wang, K. Electrochemical and Chemical Reactivity of Dithiolene Complexes, p 267. (f) Cummins, S. D.; Eisenberg, R. Luminescence and Photochemistry of Metal Dithiolene Complexes, p 315. (g) Van Houten, K. A.; Pilato, R. S. Metal Dithiolene Complexes in Detection: Past, Present and Future, p 369. (h) Faulmann, C.; Cassoux, P. Solid-State Properties (Electronic, Magnetical, Optical) of Dithiolene Complex-Based Compounds, p 399.

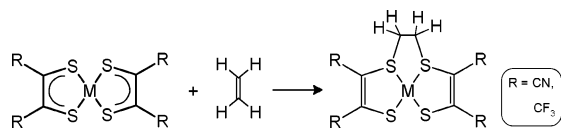
Scheme 1



The largest contributions to the highest occupied molecular orbital (HOMO) and lowest unoccupied MO (LUMO) are from atomic orbitals (AOs) based on the ligands, with smaller contributions from the metal AOs.^{1c} Complexes $\text{M}[\text{S}_2\text{C}_2\text{R}_2]_2^z$ can often undergo reversible one-electron transfer, and particularly stable forms are normally the neutral form ($z = 0$), the monoanionic form ($z = 1-$), and the dianionic form ($z = 2-$). Redox potentials for a given type of reduction (e.g., $E_{0/-1}$ for $z = 0$ and $1-$) strongly depend on R and less pronouncedly on M (Ni, Pd, or Pt). The neutral compounds are remarkably strong oxidants if they contain electron-withdrawing substituents: $E_{0/-1}$ values have the most positive values by far for $\text{R} = \text{CN}$ and CF_3 , in fact more positive than $+0.8$ V vs SCE. Phenyl derivatives ($\text{R} = \text{C}_6\text{H}_5$) are much less oxidizing, by roughly 0.5 V.^{1e} The “high-potential” (referring to $E_{0/-1}$) charge-neutral species have recently attracted increased attention because it was reported that Ni complexes with $\text{R} = \text{CN}$ and CF_3 can bind to linear alkenes in a nonconventional fashion, employing the S atoms (Scheme 2, shown for ethylene).² This discovery may hold significant technological promise for alkene separation and purification because the nickel bis(dithiolene) system is not easily poisoned by S impurities.² The Pd and Pt complexes are expected to react similarly.³ The mechanism of such alkene reactions is the topic of recent theoretical⁴ and experimental⁵ studies. Gaining deeper understanding of the

(2) Wang, K.; Stiefel, E. I. *Science* **2001**, 291, 106.

Scheme 2



properties of the highly oxidizing charge-neutral $M[S_2C_2R_2]_2$ species will aid in the development of new applications. Here, we report the first crystallographic structural determination for a high-potential metal bisdithiolene of a Ni triad metal in its neutral and pure form, for $Pt[S_2C_2(CF_3)_2]_2$ (**1**). In addition, we provide solid-state ^{195}Pt NMR data for this compound, which complement the optical^{1c,f} and vibrational^{1d,6} techniques frequently used for metal bisdithiolenes.

Most of the neutral high-potential bisdithiolenes of the Ni triad metals were first generated, often electrochemically,⁷ in the mid-1960s. The reduced forms have been extensively characterized: starting with the structural determination of $Ni[S_2C_2(CN)_2]_2^{2-}$,⁸ more than 100 crystal structures have been reported.^{1b} In contrast, very few structural characterizations of the neutral species have been reported in the literature. For $R = \text{CN}$, the neutral Ni, Pd, and Pt compounds have only recently (2001) been prepared in the form of stable solutions on a preparative scale and have not yet been isolated and characterized as solids.⁹ For $R = \text{CF}_3$, the characterization is similarly incomplete: the neutral Pd complex has not been characterized as a solid, the neutral Pt complex¹⁰ was characterized as a solid but no crystal structure exists,¹¹ and the neutral Ni complex¹² has only been characterized as a cocrystallize with perylene.¹³ While cocrystallization typically leads to charge transfer and reduction of the metal complex, the authors provided evidence that most of the compound (>95%) was not reduced in their cocrystallize.¹³ Surprisingly, none of the six homoleptic bisdithiolenes obtainable from $M = \text{Ni, Pd, or Pt}$ and $R = \text{CN or CF}_3$ has been crystallographically characterized in its pure form. This contrasts with the situation for less oxidizing bisdithiolenes such as $Ni[S_2C_2-$

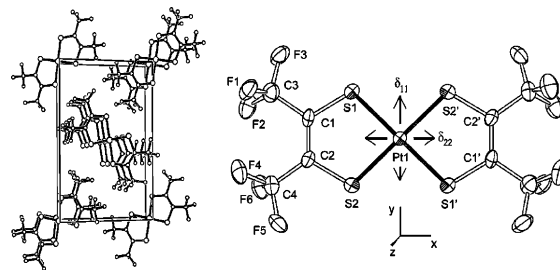


Figure 1. Crystal packing arrangement (left; view along the crystallographic a axis) and molecular structure (right) for **1**. Selected distances and angles (\AA , deg) Pt1–S1, 2.242(2); Pt1–S2, 2.236(2); S1–C1, 1.701(6); S2–C2, 1.692(6); C1–C2, 1.380(9); S1–Pt1–S2, 88.52(7); S1–Pt1–S1' (center of inversion at Pt1), 180°; S1–Pt1–S2', 91.48(7). The orientation of the ^{195}Pt NMR CS tensor (as obtained from DFT computations) is also shown: δ_{11} and δ_{22} reside in the plane of the molecule, and δ_{33} is perpendicular to this plane. A Cartesian coordinate system is defined having x , y , and z along δ_{22} , δ_{11} , and δ_{33} , respectively, to facilitate discussion (see text).

$\text{Me}_2]_2^{2-}$, where the full redox series ($z = 0, 1-, 2-$) was crystallographically characterized.¹⁴

We are currently investigating new properties of the known compound **1**.¹⁰ Using careful sublimation under vacuum,¹⁵ we obtained high-quality crystals of **1**. The single-crystal X-ray structure was solved using standard methods.¹⁶ A view of the unit cell (Figure 1) shows packing as partially interlocked stacks of molecules that form extended columns roughly parallel to the crystallographic a axis. Pt–Pt distances are very long (ca. 4.83 \AA), ruling out interatomic bonding interactions. The closest intermolecular neighbor to each Pt center is a S atom from a neighboring molecule, and at a distance of ca. 3.96 \AA , there is no intermolecular Pt–S bonding. Thus, the structure consists of closely packed monomeric **1** units. The metal is coordinated in a perfectly planar fashion (Figure 1; trans S atoms are related by a crystallographic inversion center). Deviations from ideal square geometry are due to the bis(chelate) situation, and an intra-ring S–Pt–S angle of 88.52(7)° contrasts with an inter-ring S–Pt–S angle of 91.48(7)°. The only other crystallographically characterized form of **1** is the monoanion,¹¹ **1**[−]. When corresponding bond distances are compared, it appears that the anion **1**[−] has longer Pt–S bonds and shorter C–C bonds compared to **1**, similar to the effect described for $Ni[S_2C_2\text{Me}_2]_2$:¹⁴ the Pt–S bond of **1** lengthens from 2.240(4) to 2.255(8) \AA in **1**[−], and the intraligand C–C bond shortens from 1.381(9) \AA in **1** to 1.33(3) \AA in **1**[−]. While the effect is predicted by theory¹⁴ and likely is very real, the standard errors (mainly the large standard error of the 1976 structural determination of **1**[−]) compromise the statistical significance of the comparison. The bite angle is un-

(3) For complexes having phenyl substituents ($R = \text{C}_6\text{H}_5$), alkene (norbornadiene) reactions were found for all three metals Ni, Pd, and Pt: Kajitani, M.; Kohara, M.; Kitayama, T.; Akiyama, T.; Sugimori, A. *J. Phys. Org. Chem.* **1989**, 2, 131. For the Ni system, it is known that reactions are much slower for $R = \text{C}_6\text{H}_5$, compared to $R = \text{CN}$ or CF_3 .

(4) Fan, Y.; Hall, M. B. *J. Am. Chem. Soc.* **2002**, 124, 12076.
 (5) Harrison, D. J.; Nguyen, N.; Lough, A. J.; Fekl, U. *J. Am. Chem. Soc.* **2006**, 128, 11026.
 (6) Petrenko, T.; Ray, K.; Wieghardt, K. E.; Neese, F. *J. Am. Chem. Soc.* **2006**, 128, 4422.
 (7) Olson, D. C.; Mayweg, V. P.; Schrauzer, G. N. *J. Am. Chem. Soc.* **1966**, 88, 4876.
 (8) (a) Eisenberg, R.; Ibers, J. A.; Clark, R. J. H.; Gray, H. B. *J. Am. Chem. Soc.* **1964**, 86, 113. (b) Eisenberg, R.; Ibers, J. A. *Inorg. Chem.* **1965**, 4, 605.
 (9) Geiger, W. E.; Barrière, F.; LeSuer, R. J.; Trupia, S. *Inorg. Chem.* **2001**, 40, 2472.
 (10) Davison, A.; Edelstein, N.; Holm, R. H.; Maki, A. H. *Inorg. Chem.* **1964**, 3, 814.
 (11) For a reduced form, one structure exists: $\text{Pt}[S_2C_2(\text{CF}_3)_2]_2^{2-}$ with a tetrathiafulvalinium cation: Kasper, J. S.; Interrante, L. V. *Acta Crystallogr.* **1976**, B32, 2914.
 (12) Davison, A.; Edelstein, N.; Holm, R. H.; Maki, A. H. *Inorg. Chem.* **1963**, 2, 1227.
 (13) Schmitt, R. D.; Wing, R. M.; Maki, A. H. *J. Am. Chem. Soc.* **1969**, 91, 4394.

(14) Lim, B. S.; Fomitchev, D. V.; Holm, R. H. *Inorg. Chem.* **2001**, 40, 4257.

(15) See the Supporting Information.

(16) Crystal data and structure refinement for **1**: purple needle, crystal size = 0.16 mm \times 0.10 mm \times 0.06 mm, data collection on a Nonius-Kappa CCD diffractometer using Mo $K\alpha$ (0.710 73 \AA) at 150(1) K, structure solution with direct methods, structure refinement on F^2 against all reflections, $\text{C}_8\text{F}_{12}\text{Pt}_1\text{S}_4$, $M = 647.41$, monoclinic, space group $P2_1/c$, $a = 4.8285(2)$ \AA , $b = 15.2998(8)$ \AA , $c = 10.2753(6)$ \AA , $\beta = 102.077(3)^\circ$, $Z = 2$, $V = 742.29(7)$ \AA^3 , $D_{\text{calc}} = 2.897$ g cm^{-3} , 7856 reflections collected of which 1305 were independent, $\text{GOF} = 1.027$, $R1 = 0.0317$ [data with $I = 2\sigma(I)$], $wR2 = 0.0872$ (all data).

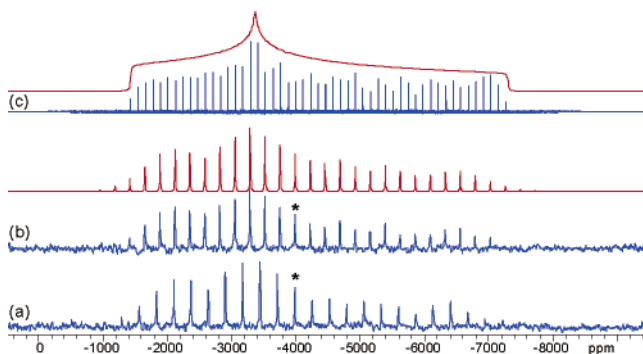


Figure 2. ^{195}Pt NMR spectra of $\text{Pt}[\text{S}_2\text{C}_2(\text{CF}_3)_2]_2$. $^{195}\text{Pt}\{^{19}\text{F}\}$ MAS single-pulse Bloch decay experiments of (a) $\nu_{\text{rot}} = 23.0$ kHz and (b) $\nu_{\text{rot}} = 20.0$ kHz (with numerical simulation) are shown using a spectral width = 850 kHz, pulse delay = 90 s, and $\text{pw}(\pi/2) = 1.0$ μs ($\nu_1 = 250$ kHz). (c) Static CP/CPMG spectrum with analytical simulation using a $\text{pw}(\pi/2) = 2.5$ μs ($\nu_1 = 100$ kHz), ^{19}F NMR matching power of 64 kHz, contact time = 7.0 ms, receiver delay = 6.0 μs , and $\tau_1 = \tau_2 = \tau_3 = \tau_4 = 20$ μs . The asterisks denote the isotropic shifts.

Table 1. Experimental and Computational CS Tensor Parameters

method	δ_{11} (ppm)	δ_{22} (ppm)	δ_{33} (ppm)	δ_{iso} (ppm) ^c	Ω (ppm), ^d κ ^e
Experimental Values					
static (CP)	-1427(50)	-3357(59)	-7277(56)	-4020(50)	5850(100), 0.34(3)
MAS: HBA 20.0 kHz	-1382(40)	-3302(80)	-7285(43)	-3990(10)	5903(75), 0.35(4)
MAS: HBA 23.0 kHz	-1378(66)	-3289(66)	-7291(83)	-3986(7)	5913(150), 0.35(3)
Computational Values, Relativistic with ZORA					
VWN + BP ^a QZ4P ^b	-505.7	-2391.1	-7365.7	-3420.8	6846.8, 0.45

^a VWN: Vosko, Wilk, and Nusair local correlation functional. BP: Becke88 exchange with Perdew86 correlation functionals.¹⁸ ^b QZ4P: quadruple- ζ basis with four polarization functions in the valence. ^c Absolute chemical shieldings (σ) are obtained from the computations [isotropic shielding is defined as $\sigma_{\text{iso}} = (\sigma_{11} + \sigma_{22} + \sigma_{33})/3$] and are converted to chemical shifts (δ_{iso}) using the formula $\delta_{\text{iso}} = (\sigma_{\text{ref}} - \sigma)/(1 - \sigma_{\text{ref}})$, where σ_{ref} is the absolute Pt shielding of the reference $[\text{PtCl}_6]^{2-}$. ^d $\Omega = \delta_{11} - \delta_{33}$. ^e $\kappa = 3(\delta_{22} - \delta_{\text{iso}})/\Omega$.

changed: $88.52(7)^\circ$ in **1** versus $88.5(5)^\circ$ in **1**⁻.¹⁷ In addition to providing an accurate molecular structure, the crystal structure proves valuable because close metal–metal contacts can be excluded, and solid-state NMR data can be interpreted in terms of intramolecular effects only.

$^{195}\text{Pt}\{^{19}\text{F}\}$ magic angle spinning (MAS) NMR spectra of $\text{Pt}[\text{S}_2\text{C}_2(\text{CF}_3)_2]_2$ (Figure 2a,b) reveal an isotropic chemical shift (CS; δ_{iso}) of ca. -3988 ppm. Using the Herzfeld–Berger (HB) analysis, Ω and κ were determined to be 5908 ppm and 0.35, respectively (Table 1). The ^{19}F – ^{195}Pt CP/CPMG static spectrum was acquired for comparison (Figure 2c) and has similar parameters, which fall within the error limits of the HB analysis (Table 1). Because CS tensor components are constrained within or near molecular symmetry elements, the most shielded component, δ_{33} , should be oriented perpendicular to the plane of the molecule.

Theoretical calculations of Pt CS tensors were performed in order to confirm the tensor orientation proposed from experimental data. Both relativistic and nonrelativistic *ADF* calculations¹⁹ show a good agreement between experimental and theoretical values of δ_{iso} (Supporting Information). However, to achieve reasonable agreement for anisotropic CS tensor parameters, relativistic effects had to be taken into

account using the ZORA²⁰ methodology (Table 1). A persistent feature of all of the calculations is the CS tensor orientation: δ_{33} is oriented along the C_2 rotational axis, while δ_{11} and δ_{22} are in the plane of the molecule, directed between and bisecting the dithiolene ligands, respectively (Figure 1). δ_{11} and δ_{22} are quite different (i.e., the CS tensor is nonaxially symmetric) in contrast to those of complexes of comparable symmetry such as $\text{Pt}(\text{acac})_2$ ²¹ and $\text{K}_2[\text{Pt}(\text{C}_2\text{O}_4)_2] \cdot 2\text{H}_2\text{O}$,²² which have skews indicating almost perfect axial symmetry and considerably larger spans. However, they are similar to those of *trans*-(Et_2S)₂ PtCl_2 , which has a first coordination sphere somewhat related to $\text{Pt}[\text{S}_2\text{C}_2(\text{CF}_3)_2]_2$ but where Pt is surrounded by “ S_2Cl_2 ” instead of “ S_4 ”.²³

A detailed MO analysis is beyond the scope of this paper, but preliminary calculations on **1** in D_{2h} symmetry indicate that δ_{11} and δ_{22} are dependent upon both the energetic spacings and the symmetries of the occupied and virtual MOs that make the largest paramagnetic deshielding contributions. These MOs are largely localized on the dithiolene ligands as opposed to the metal center, thereby producing extremely different paramagnetic shielding effects along the x and y axes (Figure 1 and Supporting Information Figure S2).

In conclusion, solid-state NMR spectroscopy can provide insight into the environment of the metal in neutral high-potential transition-metal bisdithiolenes. Despite the local axially symmetric metal environment (square-planar “ S_4 ”) in **1**, the ^{195}Pt NMR CS tensor components in the square plane clearly lack axial symmetry. This effect may become a sensitive probe for the noninnocent nature of ligands, particularly π -electron delocalization involving ligand p orbitals and metal d orbitals, which is not easily probed for diamagnetic complexes where electron spin resonance spectroscopy cannot be applied.

Acknowledgment. Funding by the Natural Science and Engineering Research Council of Canada, the Canadian Foundation for Innovation, the Ontario Research Fund, Ontario Innovation Trust, the University of Toronto, and the University of Windsor is gratefully acknowledged. We thank Neilson Nguyen for a sample of $\text{S}_2\text{C}_2(\text{CF}_3)_2$.

Supporting Information Available: Crystallographic data for **1** (CIF) and supporting text describing the synthesis and crystallization, details on NMR procedures, and details on density functional theory (DFT) computations using various methods (PDF). This material is available free of charge via the Internet at <http://pubs.acs.org>.

IC0614972

- (17) Calculated from the coordinates;¹¹ see the Supporting Information.
 (18) (a) Vosko, S. H.; Wilk, L.; Nusair, M. *Can. J. Phys.* **1980**, *58*, 1200. (b) Perdew, J. P. *Phys. Rev. B* **1986**, *33*, 8822. (c) Perdew, J. P. *Phys. Rev. B* **1986**, *34*, 7406.
 (19) (a) *ADF*, 2004.01; SCM: Amsterdam, The Netherlands, 2004. (b) Velde, G. T.; Bickelhaupt, F. M.; Baerends, E. J.; Guerra, C. F.; Van Gisbergen, S. J. A.; Snijders, J. G.; Ziegler, T. *J. Comput. Chem.* **2001**, *22*, 931. (c) Guerra, C. F.; Snijders, J. G.; te Velde, G.; Baerends, E. J. *Theor. Chem. Acc.* **1998**, *99*, 391.
 (20) (a) van Lenthe, E.; Baerends, E. J.; Snijders, J. G. *J. Chem. Phys.* **1993**, *99*, 4597. (b) van Lenthe, E.; Baerends, E. J.; Snijders, J. G. *J. Chem. Phys.* **1994**, *101*, 9783.
 (21) Dechter, J. J.; Kowalewski, J. *J. Magn. Reson.* **1984**, *59*, 146.
 (22) Keller, H. J.; Rupp, H. H. *Z. Naturforsch.* **1971**, *A26*, 785.
 (23) Ambrosius, F.; Klaus, E.; Schaller, T.; Sebald, A. *Z. Naturforsch.* **1995**, *A50*, 423.